Protist 174 (2023) 125983

Contents lists available at ScienceDirect

Protist

journal homepage: www.elsevier.de/protis

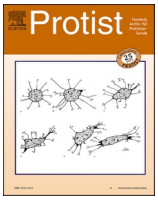

Original article

Taxonomy and morphology of *Calciopappus curvus* sp. nov. (Syracosphaeraceae, Prymnesiophyceae), a novel appendage-bearing coccolithophore

Odysseas A. Archontikis [a,b,*], Josué G. Millán [c], Harald Andruleit [d], Lluïsa Cros [e], Annelies Kleijne [f], Mikal Heldal [g], Hai Doan-Nhu [h], Amos Winter [c], Leocadio Blanco-Bercial [i], Jeremy R. Young [j]

[a] *Department of Earth Sciences, University of Oxford, South Parks Road, Oxford OX1 3AN, UK*
[b] *Department of Earth Sciences, The Natural History Museum, Cromwell Road, London SW7 5BD, UK*
[c] *Department of Earth and Environmental Systems, Indiana State University, Terre Haute, IN 47809, USA*
[d] *Bundesanstalt für Geowissenschaften und Rohstoffe (BGR), Stilleweg 2, 30655 Hannover, Germany*
[e] *Institut de Ciències del Mar, CSIC, Passeig Marítim de la Barceloneta, 37–49, E-08003 Barcelona, Spain*
[f] *Plankton Diversity and Evolution Group, Naturalis Biodiversity Center, Darwinweg 2, 2333 CR Leiden, The Netherlands*
[g] *Department of Biological Sciences, University of Bergen, Thormøhlensgate 53 A/B, 5020 Bergen, Norway*
[h] *Institute of Oceanography, Viet Nam Academy of Science and Technology, 01 Cau Da, Nha Trang, Viet Nam*
[i] *Bermuda Institute of Ocean Sciences – Arizona State University, 17 Biological Station, St. George's GE01, Bermuda*
[j] *Department of Earth Sciences, University College London, London WC1E 6BT, UK*

ARTICLE INFO

Monitoring Editor: Wiebe HCF Kooistra

Keywords:
Biodiversity
Lower Photic Zone
Morphology
Phytoplankton
Syracosphaerales
Taxonomy

ABSTRACT

Based on scanning electron microscopy observations, a new species of the coccolithophore genus *Calciopappus* (Syracosphaeraceae, Prymnesiophyceae) is described from the surface waters off Bergen and from the lower photic zone of sub-tropical and tropical waters. Morphological, coccolith rim structure and biometric analyses strongly support separation of this morphotype from the two described *Calciopappus* species, but inclusion of it within the genus. The new form differs from the other species in being noticeably smaller and in morpho-structural details of each of the three coccolith types that form the coccosphere: (1) the body coccoliths have an open central area; (2) the whorl coccoliths have a wide central opening and two thumb-like protrusions; and (3) the appendage coccoliths are curved. On this basis, the species is formally described as *Calciopappus curvus* sp. nov., its systematic affinity is discussed and compared with other extant coccolithophores.

1. Introduction

Coccolithophores (Prymnesiophyceae, Haptophyta) are single-celled photosynthetic eukaryotes that inhabit the present-day oceans and represent up to 10% of both the primary production (Poulton et al., 2007) and the global phytoplankton biomass (Tyrrell and Young, 2009). Coccolithophores produce delicately shaped calcite plates (coccoliths) to form an intricately made cell covering known as a coccosphere (Monteiro et al., 2016; Wallich, 1877). Coccolith production is an intracellular process that begins with the formation of a proto-coccolith ring (Young et al., 1999). This consists of crystal units with alternating vertically and/or radially oriented axes, known as the V/R model (Young et al., 1992), and the structure and morphology of the coccolith crystals has largely formed the basis for the development of coccolithophore taxonomy, and the elucidation of their biodiversity and evolutionary patterns.

The family Syracosphaeraceae (Syracosphaerales, Prymnesiophyceae) is one of the largest and most diverse (c. 25% of all modern species; (Young et al., 2023; Young et al., 2005)) groups of extant coccolithophores and its evolutionary root is likely placed deep within the Mesozoic divergence period (Bown et al., 2017; Medlin et al., 2008; Young et al., 2014). The family currently accommodates four morphologically distinct heterococcolith-bearing genera (Fig. 1): the type genus *Syracosphaera* Lohmann and the extant genera *Calciopappus* Gaarder & Ramsfjell *emend.* Manton & Oates, *Michaelsarsia* Gran and *Ophiaster* Gran *emend.* Manton & Oates. Presently, only members of *Syracosphaera*

* Corresponding author at: Department of Earth Sciences, University of Oxford, South Parks Road, Oxford OX1 3AN, UK.
E-mail address: odysseas.archontikis@univ.ox.ac.uk (O.A. Archontikis).

https://doi.org/10.1016/j.protis.2023.125983
Received 31 March 2023; Accepted 25 July 2023
Available online 28 July 2023

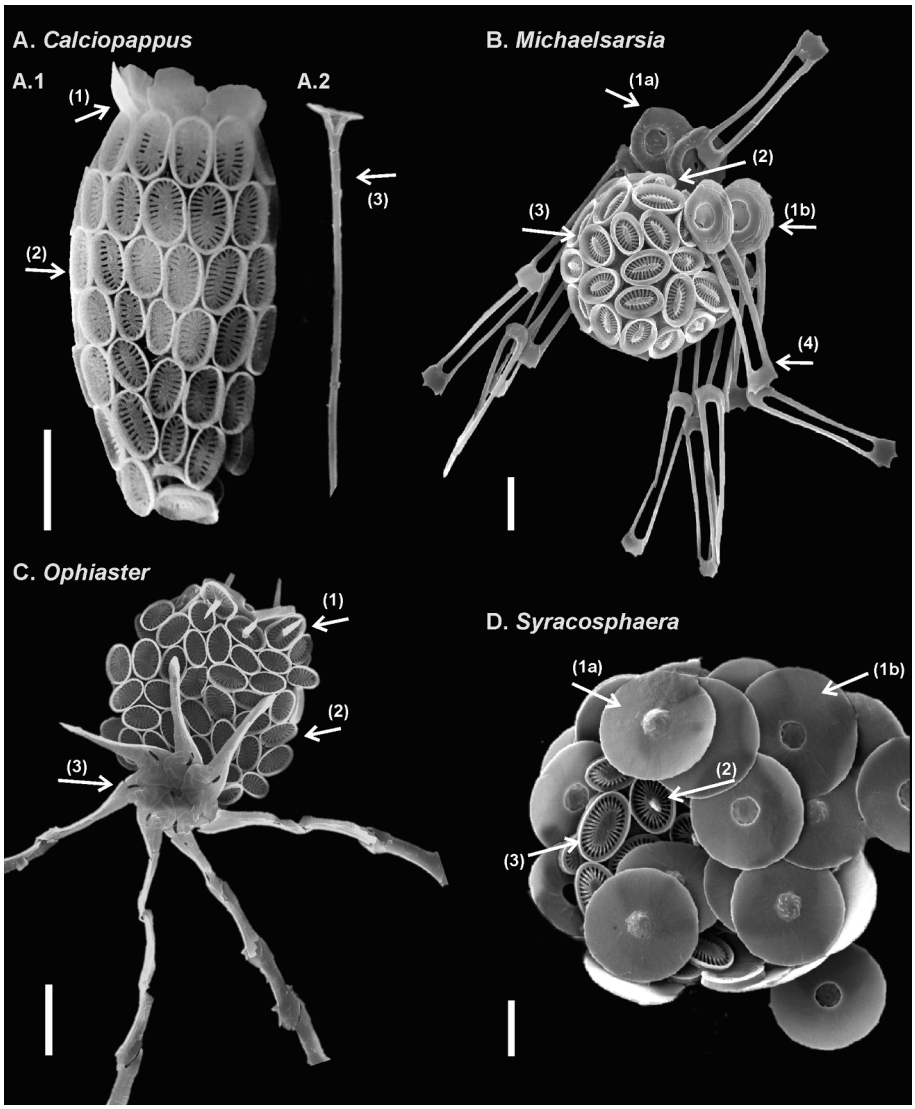

Fig. 1. Syracosphaeraceae. SEM micrographs and comparison of (A) *Calciopappus*, (B) *Michaelsarsia,* (C) *Ophiaster* and (D) *Syracosphaera* coccosphere and coccolith types. Scale bars = 2 μm. (A). *Calciopappus.* (A.1). Side view of a *C. rigidus* coccosphere deprived of appendage coccoliths but showing the ring of whorl coccoliths (arrow 1) at the flagellar opening, and body coccoliths (arrow 2) embodying the main part of the coccosphere. Arrow 1 indicates the proximal smooth side of the whorl coccoliths. Image code: 148101 (40.7764°N, 0.7497°E, November 1997, El Fangar Bay, 0–4 m; courtesy of Fortuño & Delgado). (A.2). Individual appendage coccolith of *C. rigidus* consisting of an arcuate base and a straight appendage. Image code: 7962 (Station 95MS, SO-139 cruise, –6.57°N, 104.90°E, February 1999, 50 m depth). (B). *Michaelsarsia.* SEM image of a *Michaelsarsia elegans* Gran coccosphere showing whorl coccoliths in proximal (arrow 1a) and distal (arrow 1b) views, circum-flagellar coccoliths (arrow 2), body coccoliths (arrow 3) and appendage coccoliths (arrow 4); the appendage coccoliths are attached to the whorl coccoliths. Image code: 7951 (Station 2MS, SO-139 cruise, –9.22°N, 106.29°E, February 1999, 63 m depth). (C). *Ophiaster.* SEM image of an *Ophiaster hydroideus* (Lohmann) Lohmann coccosphere consisting of circum-flagellar coccoliths (arrow 1), body coccoliths (arrow 2) and appendage coccoliths (arrow 3). The appendage coccoliths are located at the antapical pole. Image code: 7933 (Station 2MS, SO-139 cruise, –9.22°N, 106.29°E, February 1999, 63 m depth). (D). *Syracosphaera.* SEM image of a complete coccosphere of *Syracosphaera anthos* (Lohmann) Janin with exothecal planolith-type coccoliths in distal (arrow 1a) and proximal (arrow 1b) views, and endothecal circum-flagellar coccoliths (arrow 2) and body coccoliths (arrow 3). Image code: 203–11 (Station MD-04, 57.8°N, –10.2°E, 13 June 2004, R/V *Marion Dufresne*, North-eastern Atlantic, 0 m depth).

have been shown in life cycle associations with holococcolithophores (see Archontikis et al. (2020) and references therein). All four genera produce coccospheres with similar body coccoliths (Kleijne and Cros, 2009; Young et al., 2009; Young et al., 1997). These are muroliths with a rim that shows a lower/inner cycle of V-units and an upper/outer cycle of R-units (Bown et al., 2017); the R-units form an elevated wall with usually one to three lateral flanges. The central area is variable in morphology but typically formed by radial (T-unit) laths with tangential orientation of their calcite axes. The T-unit elements interdigitate with the rim units and form a disjunct cycle at the central structure (see more details in Kleijne and Cros 2009; Bown et al., 2017). In addition to the body coccoliths, *Syracosphaera* species (Fig. 1D) typically show two other types of coccoliths: circum-flagellar coccoliths and exothecal coccoliths. The circum-flagellar coccoliths are usually similar to the body coccoliths but with spines. The exothecal coccoliths form a complete or partial outer layer to the coccosphere and are highly variable in morphology being either planoliths or muroliths (Kleijne and Cros, 2009; Young et al., 2003). The exothecal planoliths show a smooth and convex distal side and a concave proximal surface (Fig. 1D). The other three genera, *Calciopappus, Michaelsarsia* and *Ophiaster*, do not have exothecal coccoliths as conventionally recognised but instead have whorl coccoliths and/or appendage coccoliths that are possibly homologous with the exothecal coccoliths (Young et al., 2009). In *Calciopappus* (Fig. 1A) and *Michaelsarsia* (Fig. 1B) the whorl coccoliths and the appendage coccoliths are disposed around the flagellar pole. The whorl coccoliths show a proximal side that is smooth and convex, and a distal side that is concave and stepped. The appendage coccoliths are formed of one or two types of highly modified coccoliths (Aubry, 2009; Manton et al., 1984; Manton and Oates, 1983; Young et al., 2009) and can be either extended forming a radial structure at the top of the coccosphere or arranged "swept back" parallel to the body of the coccosphere. Young et al. (2009) concluded that the appendages are probably formed in the swept back orientation in *Calciopappus* and *Michaelsarsia* and wrapped around the cell in *Ophiaster*, and are subsequently deployed in the extended orientation, possibly as a defence mechanism.

Gaarder and Ramsfjell (1954) formally erected the genus *Calciopappus* and its type species *Calciopappus caudatus* from the surface waters of the Northern Norwegian Sea. The species was described as "narrowly conical, with a thin antapical process" and bearing "ordinary coccoliths long-elliptical, nearly flat, narrow-rimmed; longitudinally arranged in close coaxial rings. A whorl of deviating coccoliths bearing long, thin, distally constricted spines borders the flagellar field.". An additional species, *C. rigidus,* was later proposed by Heimdal in Heimdal & Gaarder (1981, p. 42) and was discriminated from the first on the grounds of showing body coccoliths "…smaller and having a lower number of central lamellae running at nearly right angles to the elliptical outline of the coccolith". By means of light and transmission electron microscopies, Manton & Oates (1983) later demonstrated from material from

the Galapagos Islands that *Calciopappus* cells are motile with both flagella and a short haptonema. In addition, the arrangement of the appendage structures across the coccospheres of *Calciopappus, Michaelsarsia* and *Ophiaster* was shown to be different– around the flagellar opening in *Calciopappus* and *Michaelsarsia*, but at the antapical pole in *Ophiaster* (Aubry, 2009; Manton et al., 1984; Manton and Oates, 1983; Young et al., 2009).

The two formally described species of *Calciopappus, C. caudatus* Gaarder & Ramsfjell and *C. rigidus* Heimdal, are well-established, readily separable, and widely reported. In addition, one rare morphotype has previously been noted and informally proposed (Cros and Fortuño, 2002; Young et al., 2003). This form is smaller and shows body coccoliths with an open central area and curved appendage coccoliths. As in the other species of *Calciopappus,* the appendage coccoliths vary in orientation, i.e., being either extended radially or swept-back parallel to the body of the coccosphere (Figs 2, 3).

For the present work, we have assembled thirty-five scanning electron microscope (SEM) images of this morphotype from our individual collections from several environments (Fig. 4) to compare its coccolith structure with other currently known coccolithophores. Morphological, biometric and coccolith rim structure analyses support its circumscription as a new species and, therefore, it is formally described, and its systematic affinity is discussed.

2. Results

2.1. Taxonomy

Division Haptophyta Hibberd (1972) *ex.* Edvardsen & Eikrem in Edvardsen et al. (2000)

Class Prymnesiophyceae Hibberd (1976) *emend.* Cavalier-Smith et al. (1996)

Order Syracosphaerales Hay (1977) *emend.* Young et al. (2003)

Family Syracosphaeraceae (Lohmann, 1902) Lemmermann (1903)

Genus *Calciopappus* Gaarder and Ramsfjell (1954) *emend.* Manton and Oates (1983)

Species *Calciopappus curvus* Archontikis, Millán, Cros & Young sp. nov. (Figs 2C, 3C, 5–7, 11A–B).

Synonymy: *Calciopappus* sp. 1 (very small) Cros and Fortuño (2002, pp 27, 86, Figs 24C, 24D).

Calciopappus sp. Young et al. (2003, pp 32–33, Figs 14, 15).

Etymology: After Latin *curvus -a -um* (adjective), curved; referring to the distinctly curved appendage of the appendage coccoliths of the species.

Diagnosis: Species of *Calciopappus* with a monothecate coccosphere composed of c. 60–90 body coccoliths with an open central area, c. 8–12 whorl coccoliths with a central opening and two thumb-like protrusions, and c. 8–12 curved appendage coccoliths.

Holotype: Stub no. 459/3 deposited at the collections of NHM, UK (PM NF 4815 199–04). Specimen shown in Fig. 5A.

Paratype: Stub no. 459/3 deposited at the collections of NHM, UK (PM NF 3728 OA330–453). Specimen shown in Fig. 5E.

Type Locality: North-western Mediterranean and Alboran Seas (37°25.8′N, 0°25.3′W, depth 90 m, 5 October 1999, MATER-II Cruise, Station 69–6).

Distribution: Sub-tropical lower photic zone (LPZ) waters and isolated records from the tropical LPZ and North Sea surface waters.

Number of specimens studied: 35.

2.2. Description of C. curvus sp. nov.

Coccosphere. All observed coccospheres are elongate, slender and/or with an obpyriform shape, and taper progressively towards the antapical pole of the coccosphere (Figs 5–7). Coccosphere dimensions are c. 6–8 μm with swept-back appendages, parallel to the body of the coccosphere, and c. 14–18 μm with radially extended appendages. The coccospheres are monothecate and they are characterised by the presence of three types of coccoliths: (1) body coccoliths covering the main body of the coccosphere; (2) whorl coccoliths arranged in an imbricate ring around the flagellar opening showing anticlockwise imbrication; and (3) appendage coccoliths also located around the flagellar pole, and seen attached to the proximal side of the whorl coccoliths. No differentiated circum-flagellar coccoliths are observed. The number of the body coccoliths, whorl coccoliths and appendage coccoliths range, respectively, from 60 to 90, 8 to 12 and 8 to 12.

No direct observation for the presence of flagella can be made, however, on 12 out of 35 collapsed coccospheres, we have observed flagellum-like structures on the filter membranes (Figs 5F, 6A) that are similar to those observed on other coccolithophores, e.g., *Calciopappus rigidus* as imaged by Manton & Oates (1983, Fig. 42a).

Body coccoliths. The body coccoliths are predominantly minuscule, irregularly elliptical muroliths with a narrow rim (0.2 μm wide) and an open central area. The rim lacks flanges and appears to be formed of a single cycle of sub-rectangular crystals (Fig. 5H), although it is possible that a second cycle of very small units is present. Length 0.5–1.3 μm (average 0.9 μm from 698 measurements). Width 0.4–0.9 μm (average 0.6 μm from 698 measurements).

Whorl coccoliths. These are concavo-convex planoliths with an irregular but broadly sub-circular outline and a widely open central area. The rim is composed of two cycles of imbricate crystals, an inner and narrow cycle of elongate units and an outer cycle of more robust, rectangular elements (Figs 5C, 6C). The proximal side of the whorl coccoliths is convex and typically smooth (Figs 5D, 6C, 7C), whereas the distal surface is concave and stepped (Fig. 6D). Two thumb-like protrusions are developed from the outer whorl coccolith cycle, extend from its margin and taper to a fine tip (Fig. 6C, arrow 3). One of the protrusions is directed into the flagellar opening, whilst the other is directed towards the adjacent whorl coccolith, forming a tangentially anticlockwise pattern aligned with the outer edge of the ring of whorl coccoliths (Fig. 6D). Whorl coccolith length is 0.5–1.8 μm (average 1.0 μm from 152 measurements) and width is 0.2–1.5 μm (average 0.8 μm from 152 measurements).

Appendage coccoliths. The appendage coccoliths consist of an arcuate base bearing two delicate struts, each formed of a row of elongate crystals. These show dextrogyral curvature in distal view and laevogyral in proximal view. The struts merge (Fig. 6E) to form a long and distinctly curved appendage ending in a sharp tip (Fig. 7D). The base of the appendage coccoliths is 0.4–0.7 μm (average 0.6 μm from 65 measurements) long, and 0.2–0.5 μm (average 0.3 μm from 65 measurements) wide. The appendage is c. 4–6 μm long and its curvature angle is 9.9°–37.7° (average 21.9° from 119 measurements).

2.3. Biometric Analyses

To test whether *C. curvus* sp. nov. differs morphometrically from the two other described *Calciopappus* species, we carried out biometric analyses on 4226 coccoliths (3445 body coccoliths, 567 whorl coccoliths and 214 appendage coccoliths) from coccospheres of *C. caudatus, C. rigidus* and *C. curvus* sp. nov., from our collections and previously published images ((Andruleit et al., 2005; Konno and Jordan, 2006; Thomsen, 2016); see Table S1). To avoid any subjectivity in the resulting datasets, in each case we measured all the suitably oriented coccoliths. To quantify as objectively as possible the total curvature of the appendages in *C. curvus* sp. nov., we calculated the difference in the orientation between tangents to the ends of the appendage (see Fig. 8) and used this as the 'curvature angle'.

The morphometric frequency plots (Fig. 9) show clear differences between the three species with regard to the dimensions (see Table 2) of each of the three coccolith types (body coccoliths, whorl coccoliths and appendage coccoliths). In *C. curvus* sp. nov., the body coccoliths range from 0.5 μm to 1.3 μm (mean value 0.9 μm) in length and 0.4 μm to 0.9 μm (mean value 0.6 μm) in width, while whorl coccoliths are,

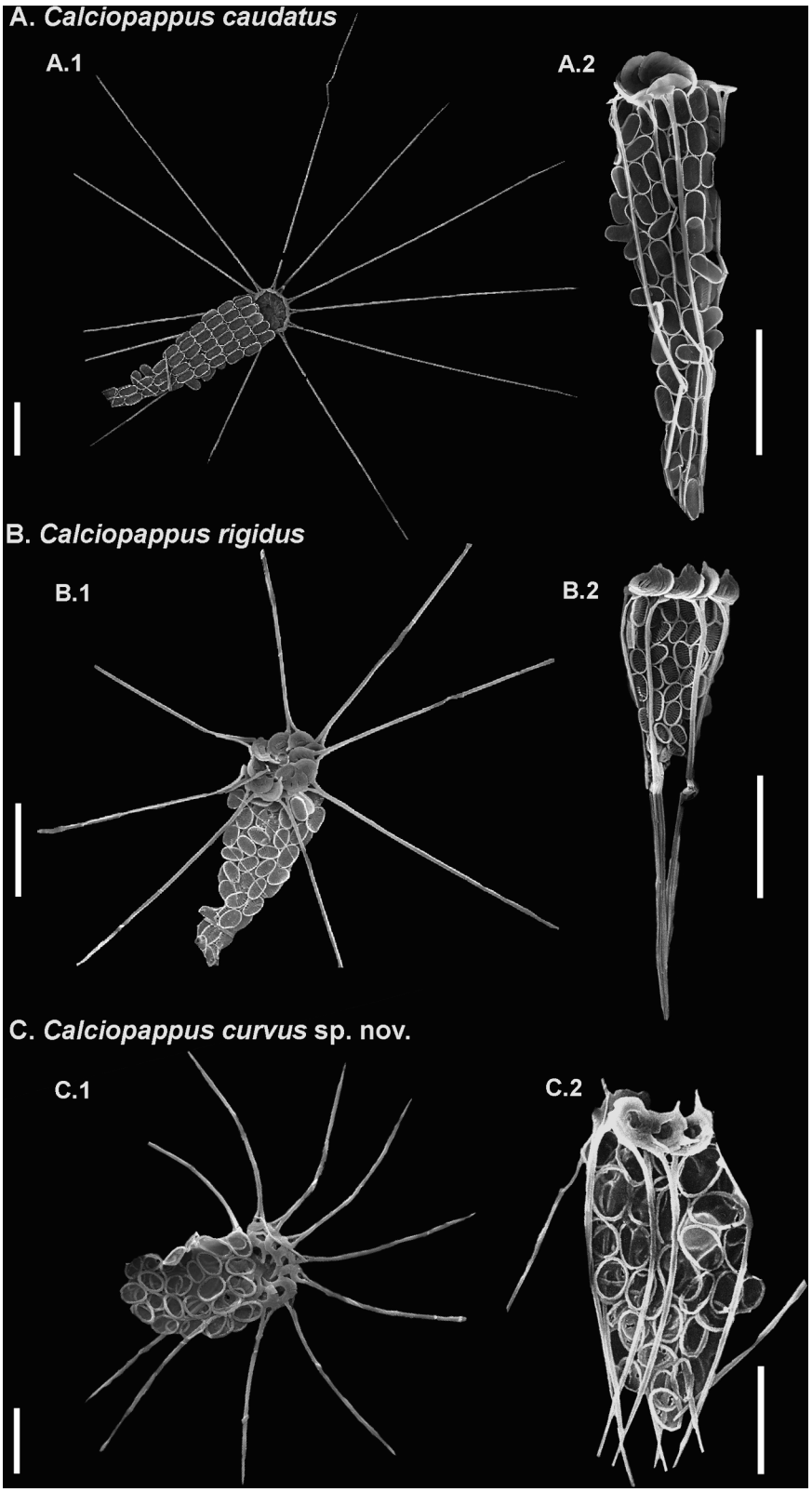

Fig. 2. Comparison and SEM micrographs of (A) *C. caudatus,* (B) *C. rigidus* and (C) *C. curvus* sp. nov. coccospheres. A.1., B.1., C.1. Well-preserved coccospheres with radially extended appendages. Image codes: 313–20, 193–62, 199–04. A.2., B.2., C.2. Coccospheres with swept-back appendages parallel to the body of the coccosphere. Image codes: 5180, 2420, 140807. Scale bar = 5 μm (Figs A.1, A.2, B.1, B.2) and 2 μm (Figs C.1, C.2).

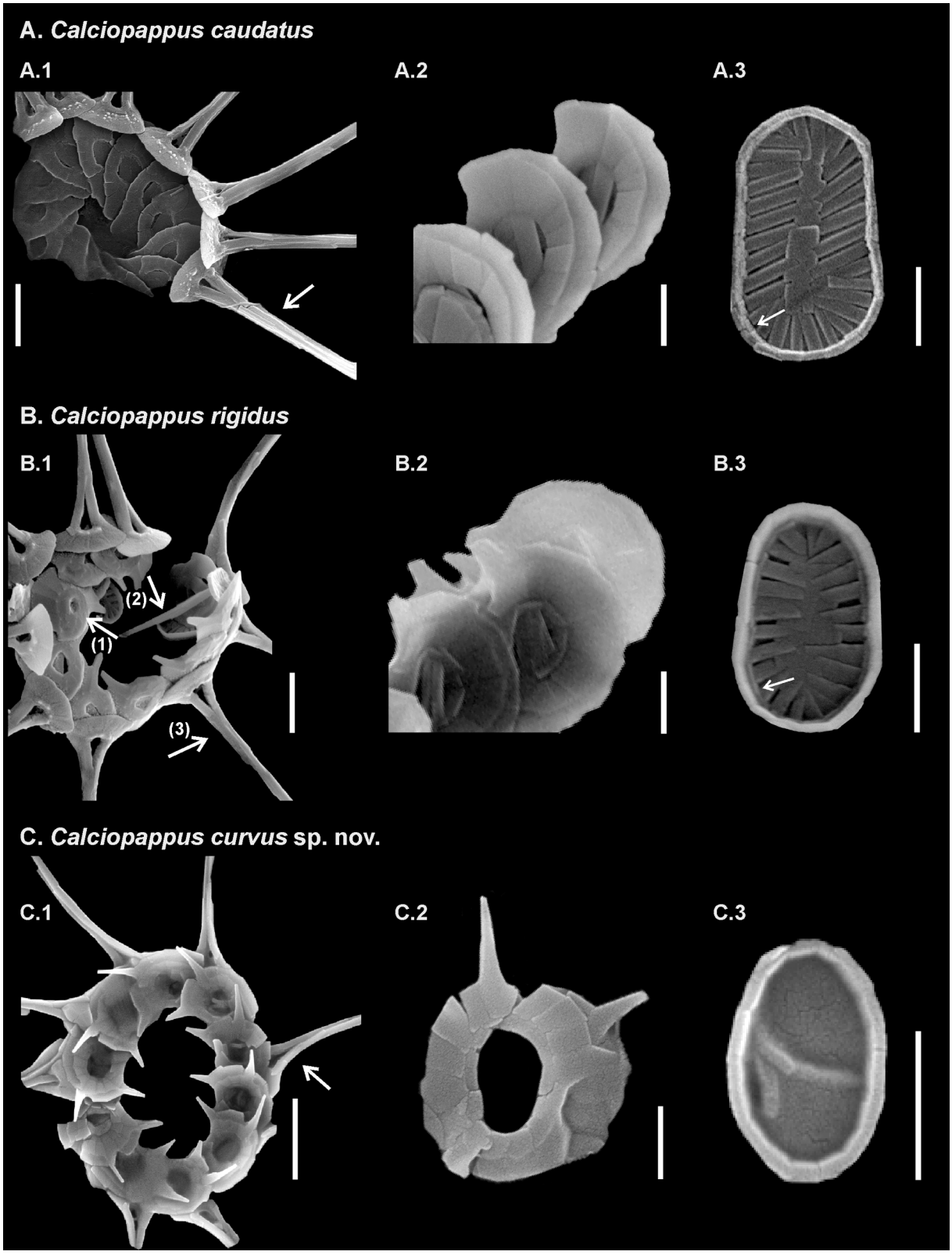

(caption on next page)

Fig. 3. SEM micrographs and comparison of body coccoliths, whorl coccoliths and appendage coccoliths of (A) *C. caudatus,* (B) *C. rigidus* and (C) *C. curvus* sp. nov. Scale bar = 1 μm (Figs A.1, B.1, C.1.) and 0.5 μm (Figs A.2, A.3, B.2, B.3, C.2, C.3). (A). *C. caudatus.* (A1). Imbricate ring of whorl coccoliths and appendage coccoliths. Whorl coccoliths with a central opening covered by elements and no thumb-like projection, observed in proximal view. Appendage coccoliths with an arcuate base and a straight appendage (arrow). Image code: 07204 (Bergen Fjord; 60.40°N, 5.3°E; 0 m depth). (A2). Distal view of whorl coccoliths. Image code: 135–04. (Station 69, 37.4301°N, –0.4199°E, October 1999, North-western Mediterranean & Alboran Seas, R/V *Hesperides,* 42.5 m depth). (A3). Body coccolith showing laths with sinistral obliquity and two cycles of rim elements (arrow). Image code: 324–034 (Sample JRY271-CTD56, 71.740°N, 8.442°E, June 2012, Arctic Ocean, 20 m depth). (B). *C. rigidus.* (B1). Ring formed of whorl coccoliths and appendage coccoliths, and the circum–flagellar coccolith. Whorl coccoliths with a central opening covered by elements, and one thumb-like projection, observed in their proximal side (arrow 1); circum-flagellar coccolith with a central spine (arrow 2). Appendage coccoliths with an arcuate base and a straight appendage (arrow 3). Image code: 221–04 (Station 69–11, 37.430°N, –0.4199°E, October 1999, North-western Mediterranean & Alboran Seas, R/V *Hesperides,* 42.5 m depth). (B2). Whorl coccolith distal side. Image code: 6502 (Station GeoB10045-2, –8.477°N, 109.021°E, 23 August 2005, South-eastern Indian Ocean, R/V *Sonne,* 55 m depth). (B3). Body coccolith with laths radially oriented and two cycles of rim elements (arrow). Image code: 135–10 (Station 69, 37.4301°N, –0.4199°E, North-western Mediterranean & Alboran Seas, R/V *Hesperides*, 42.5 m depth). (C). *C. curvus* sp. nov. (C1). Imbricate ring with whorl coccoliths and appendage coccoliths. Whorl coccoliths with a wide central opening and two thumb-like projections in distal view. Appendage coccoliths with an arcuate base and a curved appendage (arrow). Image code: 6423. (C2). Proximal view of a whorl coccolith. Image code: 6157. (C3). Body coccolith with an open central area and one cycle of rim elements. Image code: 6423.

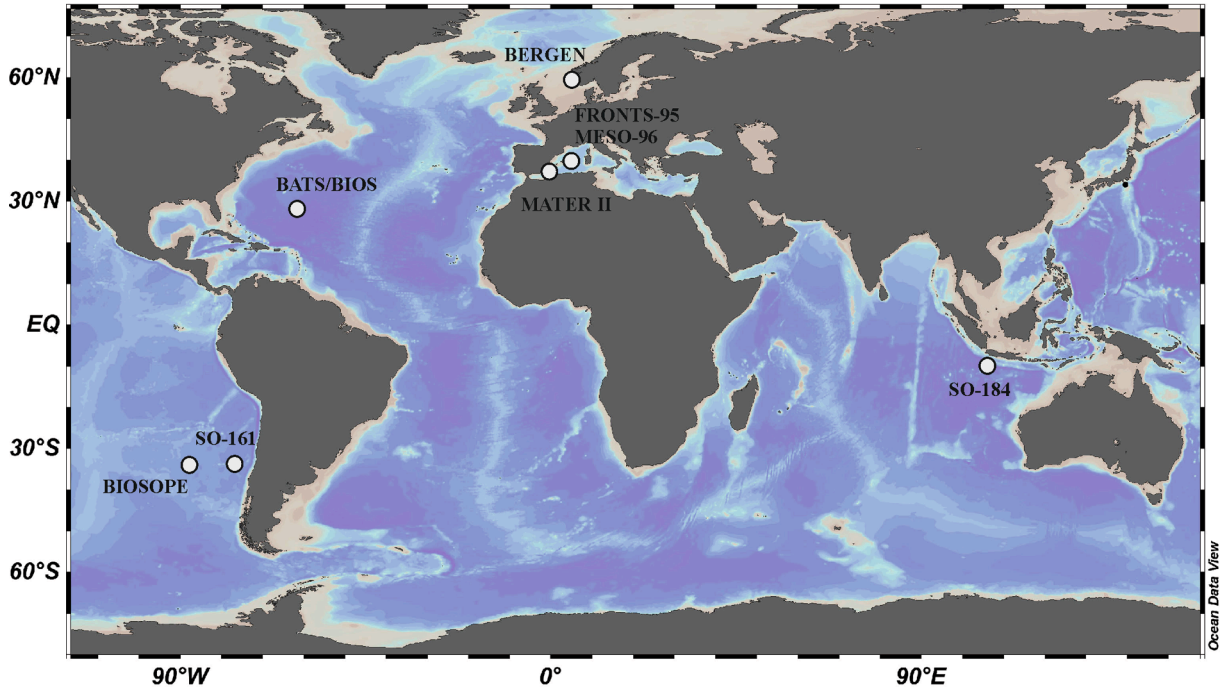

Fig. 4. Map of the locations in which *Calciopappus curvus* sp. nov. specimens were found. Map is generated using the software OceanDataView v. 5.5 (Schlitzer, 2021).

respectively, 0.5–1.8 μm (mean value 1.0 μm) long and 0.2–1.5 μm (mean value 0.8 μm) wide. The appendage coccoliths in *C. curvus* sp. nov., span 0.4–0.7 μm (mean value 0.6 μm) in length and 0.2–0.5 μm (mean value 0.3 μm) in width, while their curvature angle ranges from 9.9° to 37.7° (mean value 21.9°). In *C. rigidus,* body coccoliths are 0.7–1.9 μm (mean value 1.3 μm) long and 0.4–1.5 μm (mean value 0.9 μm) wide. The length and width of the whorl coccoliths are measured at, respectively, 0.7–1.8 μm (mean value 1.3 μm) and 0.4–1.6 μm (mean value 1.1 μm), while appendage coccoliths demonstrate length and width values ranging, respectively, from 0.9 μm to 1.5 μm (mean value 1.2 μm) and 0.3 μm to 0.8 μm (mean value 0.6 μm). In *C. caudatus,* body coccolith length and width are measured, respectively, at 1.0–2.0 μm (mean value 1.6 μm) and 0.5–1.2 μm (mean value 0.8 μm). The whorl coccoliths range from 0.7 μm to 1.9 μm (mean value 1.4 μm) in length, and 0.5 μm to 1.5 μm (mean value 1.0 μm) in width. In relation to the appendage coccoliths, these are 0.7–1.3 μm (mean value 1.0 μm) long and 0.3–0.7 μm (mean value 0.4 μm) wide in *C. caudatus*. We therefore observed that *C. curvus* sp. nov., is noticeably smaller in all coccolith types compared to both *C. rigidus* and *C. caudatus*.

3. Discussion & Conclusions

3.1. Morphological diversity in Calciopappus

Calciopappus curvus sp. nov. differs substantially from *C. caudatus* and *C. rigidus* in terms of morphology and biometry, and, therefore, warrants its circumscription as a distinct species. However, it is equally evident that the combination of its morphological characteristics fits the main diagnostic features of *Calciopappus* (Cros and Fortuño, 2002; Gaarder et al., 1954; Gaarder and Ramsfjell, 1954; Heimdal and Gaarder, 1981; Manton and Oates, 1983; Young et al., 2009; Young et al., 2003), i.e., monothecate coccospheres formed of (1) body coccoliths with a narrow murolith-type rim and a central area; (2) imbricate planolith-type whorl coccoliths forming a ring; and (3) appendage coccoliths with an arcuate base and a distinctly long appendage. In comparison to *C. caudatus* and *C. rigidus* (see Table 2; Figs 2, 3), whose body coccoliths are characterised by a central area floored by slightly overlapping lath units, *C. curvus* sp. nov., shows body coccoliths that are noticeably smaller (Fig. 9) and with no central area calcification at all. In addition, in

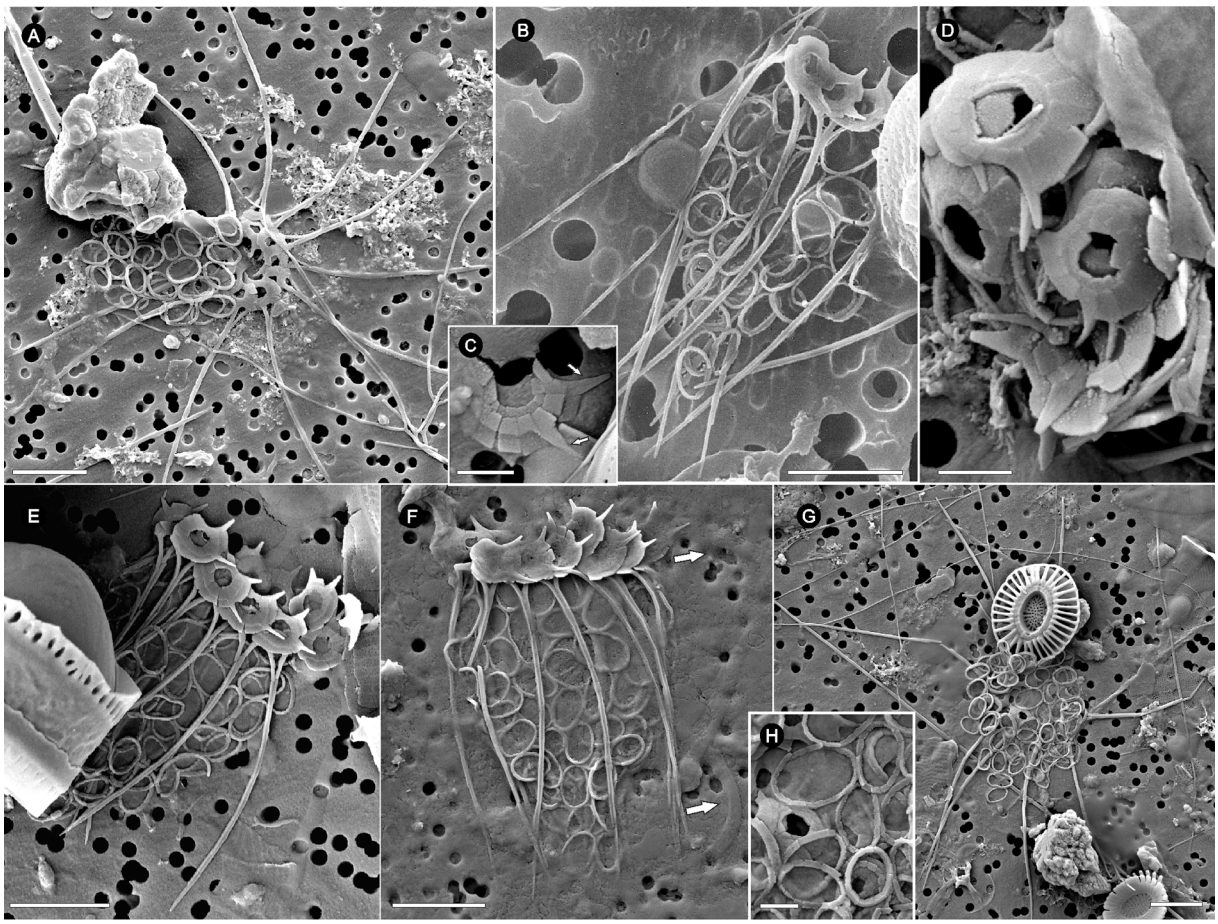

Fig. 5. SEM micrographs of *Calciopappus curvus* sp. nov., from the North-western Mediterranean and Alboran Seas. Scale bar = 2 μm (Figs A, B, E–G) and 0.5 μm (Figs C–D, H). (A). Holotype. Coccosphere showing (1) a ring of imbricate whorl coccoliths; (2) appendage coccoliths with a curved appendage and an arcuate base that is attached to (or loosely detached from) the whorl coccoliths; and (3) lightly calcified body coccoliths forming the main part of the coccosphere. Image code: 199–04. (B). Coccosphere with swept-back appendage coccoliths that curve around the main body of the coccosphere forming a narrow cone. Image code: 140807. (C). Detailed view of a whorl coccolith showing the stepped distal but flattened side and two thumb-like protrusions (arrows). Image code: OA330–459. (D). Detailed image of whorl coccoliths showing the smooth, convex, proximal side; bottom whorl coccolith in stepped distal view. Image code: OA330–463. (E). Paratype. Coccosphere elongate and broad with swept-back appendage coccoliths. Image code: OA330–453. (F). Complete coccosphere. Arrows indicate the presence of flagellum-like structures. Image code: OA330–539. (G). Collapsed coccosphere in antapical view showing body coccoliths and appendage coccoliths, and a *G. huxleyi* (see Bendif et al. (2023)) coccolith. Image code: OA330–514. (H). Detail of Fig. G, showing the simple ring morphology of the body coccoliths and a whorl coccolith in its proximal view.

C. caudatus and *C. rigidus*, the body coccolith rim is clearly formed of two cycles of units (Figs 3A.3, 3B.3, 10E, 10F) whereas in *C. curvus* sp. nov., it appears to have been reduced to a single cycle (Fig. 3C.3). The whorl coccoliths overlap slightly and form an anticlockwise imbricate ring around the flagellar opening similar to those of *C. caudatus* and *C. rigidus* (Gaarder and Ramsfjell, 1954; Manton and Oates, 1983). These show a central and sub-circular opening and two thumb-like protrusions (Figs 3C, 6C) in the exterior edge of their outer cycle, as opposed to both *C. rigidus* and *C. caudatus,* in which, whorl coccoliths have one and no thumb-like projection, respectively. When examining the appendage coccoliths, it also appears that the three known species are remarkably similar, all consisting of an arcuate base with two crystal-made struts that merge progressively to form an appendage. However, in *C. curvus* sp. nov., the appendage differs in that it becomes increasingly curved after the two struts merge (Fig. 7D), whereas appendages of *C. rigidus* and *C. caudatus* coccoliths are straight (Gaarder & Ramsfjell, 1954; Heimdal & Gaarder, 1981; Manton & Oates, 1983; Young et al., 2009). No circum-flagellar coccolith that is analogous to the one in *C. rigidus* (Fig. 3B.1) is observed in *C. curvus* sp. nov. It should finally be noted that neither life cycle observations involving members of *Calciopappus* nor molecular genetic data are currently available for the genus. Chloroplasts are clearly visible by light microscopy in the other species of *Calciopappus* (Manton & Oates, 1983; our observations) and so, it is likely they are also present in *C. curvus* sp. nov.

3.2. Ultrastructure in C. curvus sp. nov. and Calciopappus

As discussed in Inouye and Pienaar (1988), Young et al. (2004) and Bown et al. (2017), body coccoliths of species of *Syracosphaera* and *Calciopappus, Michaelsarsia* and *Ophiaster* have similar coccolith structures with a simple and narrow murolith-type rim and a central area, and therefore, they are all included in the Syracosphaeraceae (Jordan et al., 2004; Young et al., 2003). The rim structure is best known from the species *Syracosphaera pulchra* Lohmann and *Ophiaster formosus* Gran (Bown et al., 2017; Young et al., 2003; Young et al., 2004; our Fig. 10). In both species, the rim is formed of two cycles of elements. An upper/outer cycle of R-unit elements that usually form the main part of the rim, and a lower/inner cycle of V-units. In *S. pulchra,* the V-units are well-

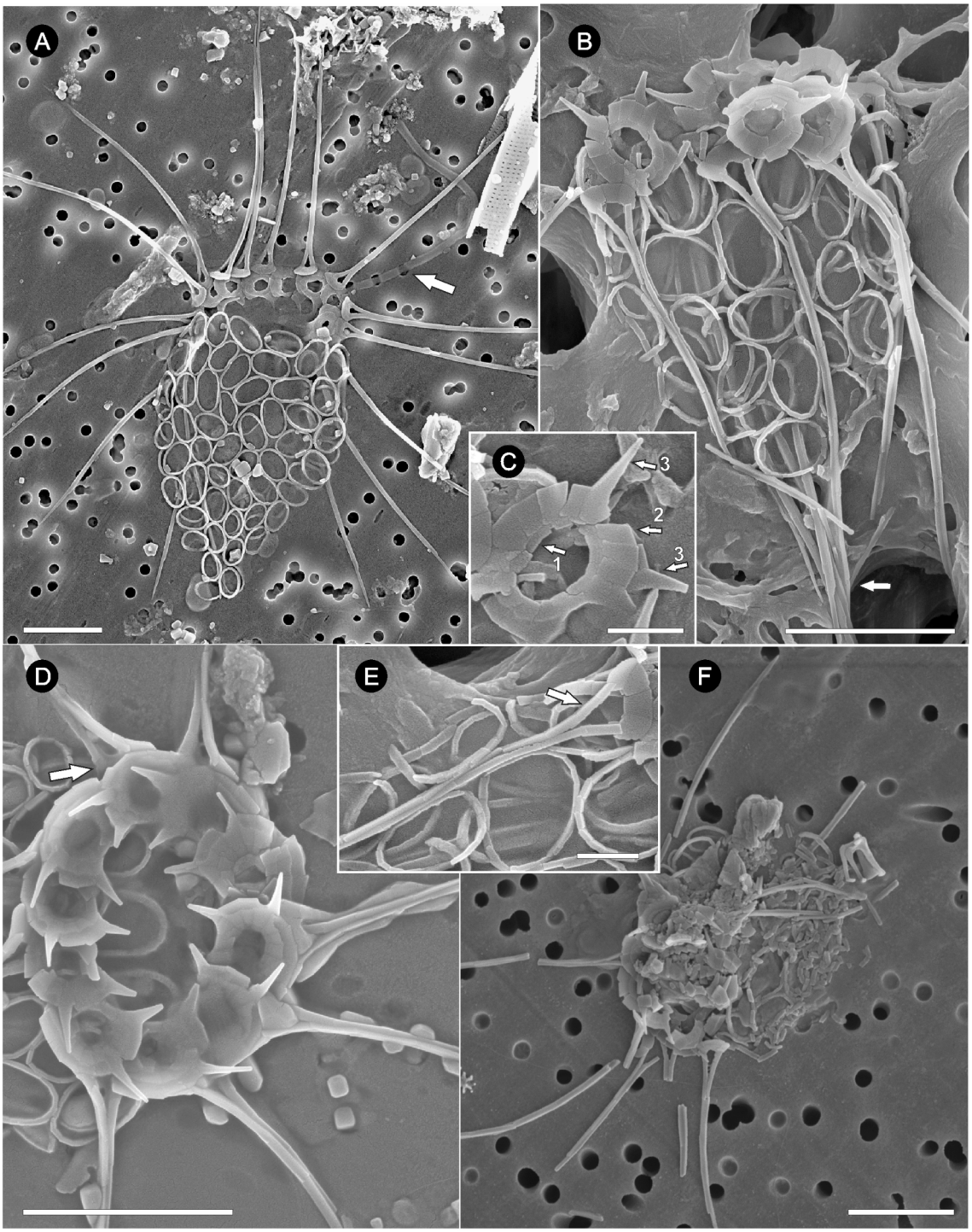

Fig. 6. SEM micrographs of *Calciopappus curvus* sp. nov., from the south-eastern Indian (Figs A, D) and Pacific Oceans (Figs B–C, E–F). Scale bar = 2 μm (Figs A–B, D, F) and 0.5 μm (Figs C, E). (A). Coccosphere elongate and broad becoming tapering antapically. It shows lightly calcified body coccoliths, whorl coccoliths and radially disposed appendage coccoliths. Arrow indicates a flagellum-like structure. Image code: 6508. (B). Complete coccosphere with body coccoliths, whorl coccoliths and appendage coccoliths. The appendage coccoliths are swept-back surrounding and extending beyond the tapered main body of the coccosphere (arrow). Image code: 6157. (C). Detail of Fig. B. Proximal view of a whorl coccolith showing a central opening and a rim consisting of an inner cycle (arrow 1) of short elongate crystals and an outer cycle (arrow 2) of rectangular elements. Two thumb–like spinous projections (arrow 3) are formed from elements of the outer cycle of the coccolith. (D). Well preserved coccosphere in apical view, with an imbricate ring of whorl coccoliths in distal view. Arrow indicates the position of an appendage coccolith underneath the whorl ring. Image code: 6423. (E). Detail of Fig. B. Appendage coccolith with an arcuate base and two struts that merge (arrow) to form an appendage. (F). Collapsed coccosphere with parts of body coccoliths, whorl coccoliths and appendage coccoliths. Upper right side with broken elements of a *G. huxleyi* coccolith. Image code: 212–12.

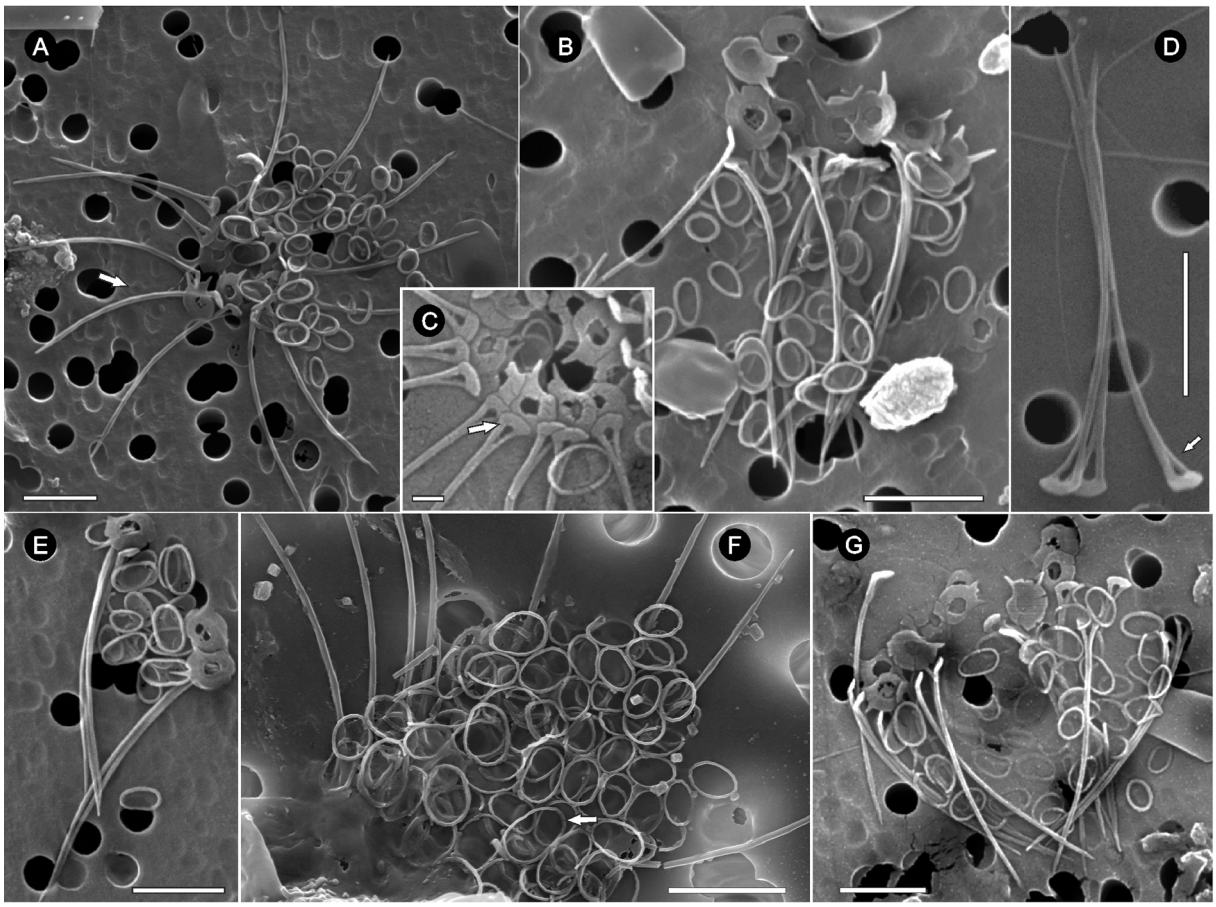

Fig. 7. SEM micrographs of *Calciopappus curvus* sp. nov. from the Sargasso Sea (Figs A–E, G) and off Bergen, Norway (Fig. F). Scale bar = 2 μm (Figs A–B, D–G) and 0.5 μm (Fig. C). (A). Collapsed coccosphere with all three coccolith types: body coccoliths as simple rings, whorl coccoliths, and appendage coccoliths whose appendage is noticeably curved (arrow). Image code: GF374C14_155m_JM56. (B). Swept-back coccosphere that tapers antapically. Image code: GF374C14_155m_JM17. (C). Detailed view of a detached ring of imbricate whorl coccoliths and appendage coccoliths (arrow). The whorl ring is observed in antapical view and the proximal, smooth side of the whorl coccoliths shows protrusions in a clockwise pattern. Image code: AB2019_80m_JM3. (D). Three appendage coccoliths. Arrow indicates the appendage coccolith base connected to two struts that progressively meet and jointly form a curved appendage. Image code: HS1391C3_1500X_170m_JM423. (E). Fragment of a coccosphere with body coccoliths, whorl coccoliths and three appendage coccoliths. Image code: AB2019_140m_JM19. (F). Well-preserved coccosphere with lightly calcified body coccoliths with a rim of a single ring of crystallites (arrow). The body coccoliths cover the appendage coccoliths which, however, show noticeably curved appendages. Image code: Calciopunknown1. (G). Collapsed swept-back coccosphere. Image code: AB2019_80m_JM5.

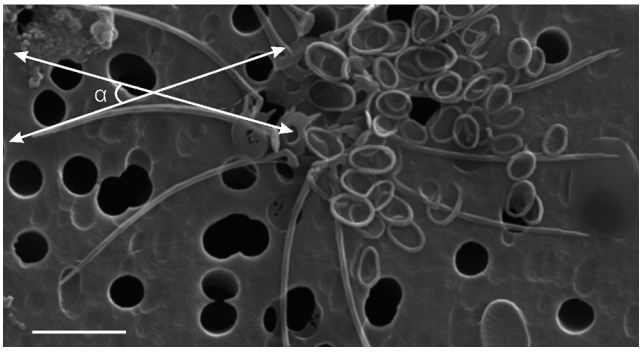

Fig. 8. Technique for measuring the total curvature of the appendages in *C. curvus* sp. nov. The angle (α°) of curvature is calculated as the difference in orientation between tangents to the ends of the appendage. Scale bar = 2 μm. Image code: GF374C14_155m_JM56.

developed, forming much of the rim including the basal and median flanges, whilst in *Ophiaster* they are much smaller forming a low basal cycle. In plan view, the V-units are weakly birefringent with sub-vertical c-axis orientation, while the R-units show radial crystallographic orientation and are strongly birefringent under polarising light (e.g., Young et al., 2004; Bown et al., 2017; our observations). The V-units form the base of the rim but a zone of alternation of V- and R-units occurs above this and is the likely locus of the proto-coccolith ring. It has been inferred that all members of the Syracosphaeraceae have similar rim structure; however, this has not been demonstrated in most cases, primarily because in small coccoliths from plankton samples, organic material usually obscures the base of the coccoliths in SEM.

Calciopappus caudatus and *C. rigidus* obviously have similar rim structures (Figs 3A.3, 3B.3) but a better developed inner rim cycle is observed in *C. caudatus*. The structure, however, is only easily visible in two high resolution transmission electron micrographs of *C. rigidus* (Figs 10E, 10F). These images clearly show that the species has a structure essentially identical to that of *Ophiaster* (Figs 10A, 10B), which Bown et al. (2017) considered to be the typical Syracosphaeraceae structure. In *C. curvus* sp. nov. however, the basal V-units cannot be

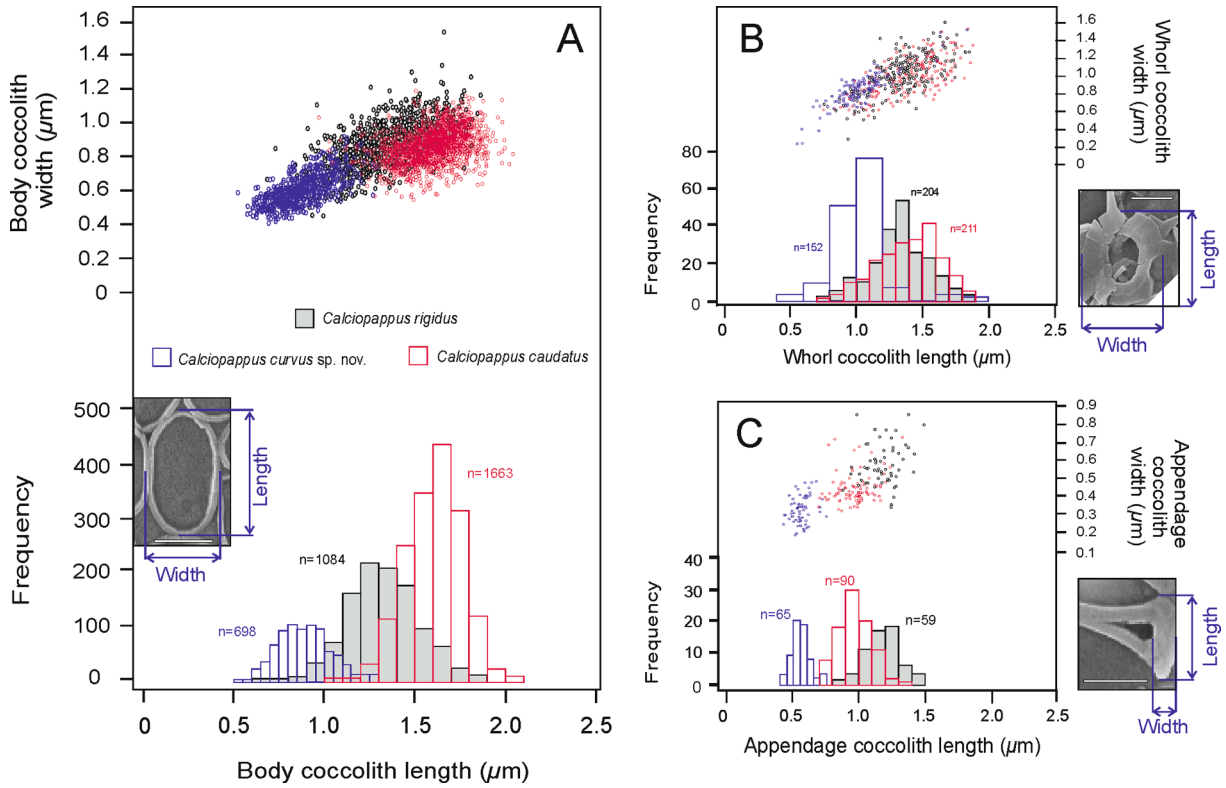

Fig. 9. Length and width measurements of (A) body coccoliths, (B) whorl coccoliths and (C) appendage coccoliths. On each sub-figure, data for *C. curvus* sp. nov. is shown in blue, *C. rigidus* in grey, and *C. caudatus* in red. SEM images show where the measurements were taken. Scale bars = 0.5 μm.

unambiguously distinguished in any of our SEM micrographs. Therefore, it appears that the V-units are either absent, or, more likely, significantly reduced in *C. curvus* sp. nov. This pattern is commonly observed in smallest murolith-type coccoliths (see section below), in which the rim is simplified, the central area structures are greatly reduced or lost completely and as a result, the coccoliths may look almost identical in morphology.

3.3. Similarities of *C. curvus* sp. nov. to other extant coccolithophores

Rather strikingly, *Calciopappus curvus* sp. nov., appears to show similarities in its body coccoliths to those of some other extant coccolithophores, namely *Ophiaster minimus* Manton & Oates, *Pseudowigwamma scenozonion* (Thomsen) Thomsen, members of the genus *Wigwamma* Manton, Sutherland & Oates (*W. annulifera* Manton, Sutherland & Oates, *W. antarctica* Thomsen, and *W. armatura* Thomsen) and *Jomonlithus littoralis* Inouye & Chihara. All these are characterised by the presence of almost identical, in morphology and size, body coccoliths that are simple rings with a central area showing no calcification (Inouye and Chihara, 1983; Manton and Oates, 1983; Manton et al., 1977; Probert et al., 2014; Thomsen, 1980; Thomsen et al., 1988; Thomsen et al., 2013). Yet, all of them differ from *C. curvus* sp. nov., in numerous ways (Fig. 11). First, in *Ophiaster minimus,* the body coccoliths are simple rings with a rim that bears an additional, proximal cycle of microcrystals (Fig. 11D), the whorl coccoliths are entirely absent (in both *O. minimus* and the genus *Ophiaster*), and there are circum-flagellar coccoliths, all showing a short spine supported by an axial cross (Fig. 11C). The circum-flagellar coccoliths are located near the flagellar opening and are perpendicular to the position of the appendage coccoliths surrounding the antapical pole across the coccosphere (Gaarder, 1967; Manton et al., 1977; Young et al., 2009). In addition, the appendage coccoliths in *Ophiaster* are formed of strings of coccoliths, termed osteoliths, and they demonstrate a rather rectangular shape (Keuter et al., 2021; Manton et al., 1977; Young et al., 2009) as opposed to a thin appendage with a fine tip. Second, the species *P. scenozonion*, which is the type species of the genus *Pseudowigwamma* Thomsen, is characterised by coccospheres that are monothecate and monomorphic consisting of body coccoliths that are simple rings. These, however, demonstrate a rather hoop-like shape and a rim formed of single rod-shaped crystallites that may occasionally show an additional quadrate element projected outwards (Thomsen, 1980; Thomsen et al., 2013). Third, *Wigwamma annulifera, W. antarctica* and *W. armatura* are also similar in bearing simple rings as body coccoliths; their rim, however, is made by two rings (Fig. 11F) of rod-shaped crystals (Thomsen et al., 1988; Thomsen et al., 2013), not one as in body coccoliths of *Calciopappus curvus* sp. nov., and the coccospheres are predominantly dimorphic with simple-ring body coccoliths but also circum-flagellar coccoliths showing a wigwam-like structure (Manton et al., 1977; Thomsen et al., 2013). Lastly, *J. littoralis,* the type species of the genus *Jomonlithus* Inouye & Chihara, is characterised by a monothecate coccosphere that consists of one type of monomorphic, small oval coccoliths with a rim and an open central area (Inouye and Chihara, 1983; Probert et al., 2014). The rim is formed of single cubic-like crystal elements (Fig. 11H) and it develops into a distal and a slight proximal flange

Table 1
List of all sampling locations, including environmental parameters, from which specimens of *Calciopappus curvus* sp. nov. were observed.

Study Area	Station	Sampling Date	Latitude (°N)	Longitude (°E)	Sampling Depth (m)	Temperature (°C)	Salinity (psu)	Conductivity (S/m)	Dissolved Oxygen (μmol/kg)	NO^{3-} (μmol/L)	PO4 (μmol/L)	Seawater Vol. Filtered (L)	Number of Specimens Studied	Figures
Northwestern Mediterranean & Alboran Seas														
FRONTS-5	24W	22-06-1995	40.565	2.645	70							0.5	1	
MESO-96	E8	02-07-1996	40.918	3.610	100							0.5	1	2C.2, 5B
MATER II	69–6	05-10-1999	37.430	–0.422	90							1	5	2C.1, 5A, 5C, 5D, 5E, 5F, 5G, 5H
Eastern Pacific Ocean														
BIOSOPE	CTD184	02-12-2004	–32.680	–84.070	105	13.89	34.12		241.35			c. 1	1	6F
SO-161/5	108MS	20-01-2002	–38.346	–74.163	73							2	1	3C.2, 6B, 6C, 6E
Indian Ocean														
SO-184/3	GeoB10044-2	22-08-2005	−8.499	109.014	100	15.4	34.51		261.7	16.39	0.93	4.5	1	3C.1, 3C.3, 6D
	GeoB10045-2	23-08-2005	−8.744	109.021	80	16.7	34.48		262.7	15.09	0.617	4	1	6A
North Sea														
Bergen	Alge-26	10-2008	60.400	5.300	0							0.5–1.5	1	7F, 11A, 11B
Sargasso Sea														
BATS-BIOS	Hydrostation ‘S’	14-10-2020	32.170	–64.500	110	20.82	36.74	5.09	218.32			8	3	
	Hydrostation ‘S’	14-10-2020	32.170	–64.500	130	20.14	36.72	5.02	209.27			8	1	
	Hydrostation ‘S’	14-10-2020	32.170	–64.500	150	19.72	36.69	4.97	203.22			8	1	
	Hydrostation ‘S’	14-10-2020	32.170	–64.500	170	19.47	36.67	4.95	200.53			8	3	7D
	Hydrostation ‘S’	26-10-2020	32.166	–64.499	155	19.40	36.66	4.94	205.96			2	2	7A, 7B
	Hydrostation ‘S’	26-10-2020	32.166	–64.499	175	19.24	36.66	4.92	206.59			2	1	
	Hydrostation ‘S’	22-11-2020	32.166	–64.499	80	21.02	36.74	5.12	208.94			2	6	7C, 7G
	Hydrostation ‘S’	22-11-2020	32.212	−64.525	120	20.28	36.71	5.03	204.03			2	2	
	Hydrostation ‘S’	22-11-2020	32.212	−64.525	140	19.80	36.68	4.98	204.61			2	1	7E
	Hydrostation ‘S’	22-11-2020	32.212	−64.525	160	19.48	36.67	4.95	204.66			2	3	
										Total			**35**	

Table 2
Diagnostic features and dimensions of the coccosphere and three coccolith types (body coccoliths, whorl coccoliths and appendage coccoliths) of all currently known *Calciopappus* species.

	Extant Species in *Calciopappus*		
Diagnostic Features & Dimensions	*Calciopappus caudatus*	*Calciopappus rigidus*	*Calciopappus curvus* sp. nov.
Coccosphere	Caudate, usually elongate and tapering.	Usually obpyriform, broader and less elongate (compared to *C. caudatus)*.	Small, lightly calcified and broad.
Diameter, µm (extended)	25–45	20–32	14–18
Diameter, µm (swept-back)	12–18	10–14	6–8
Body Coccoliths	Parallel sided, oblong, with laths showing strong sinistral obliquity. An inner rim wall is usually visible.	Irregularly elliptical showing laths oriented almost radially. An inner rim wall is visible but very low.	Narrowly, irregularly elliptical, minuscule with open central area. An inner rim wall is not visible, but probably present.
Number of body coccoliths	c. 70–100	c. 55–100	c. 60–90
Length, µm	1.0–2.0	0.7–1.9	0.5–1.3
Width, µm	0.5–1.2	0.4–1.5	0.4–0.9
Whorl Coccoliths	Concavo-convex with a central opening but no projection.	Concavo-convex with a central opening and one thumb-like projection.	Concavo-convex with a central opening and two short thumb-like projections.
Number of whorl coccoliths	c. 8–14	c. 8–12	c. 8–12
Length, µm	0.7–1.9	0.7–1.8	0.5–1.8
Width, µm	0.5–1.5	0.4–1.6	0.2–1.5
Appendage Coccoliths	Arcuate base with a straight, long appendage.	Arcuate base with a straight, long appendage.	Arcuate base with a thin and distinctly curved appendage.
Number of appendage coccoliths	c. 8–14	c. 8–12	c. 8–12
Length of base, µm	0.7–1.3	0.9–1.5	0.4–0.7
Width of base, µm	0.3–0.7	0.3–0.8	0.2–0.5
Curvature angle, °	0	0	c. 10–40°
Circum-flagellar Coccoliths	Not present.	One with a central spine.	Not present.
Length, µm	n/a	0.9–1.4	n/a
Width, µm	n/a	0.2–1.0	n/a

(Inouye and Chihara, 1983; Probert et al., 2014), as opposed to *C. curvus* sp. nov., in which body coccoliths do not bear flanges. Consequently, and based on the above, *C. curvus* sp. nov., is readily identifiable and separable from other living coccolithophores, although identification of the species and its body coccoliths should be treated with caution, especially when the other coccolith types are absent from the coccosphere.

3.4. Ecology

When scrutinising the environmental data of our studied samples, it becomes clear that *Calciopappus curvus* sp. nov., is found almost exclusively in the sub-tropical open-ocean waters, and usually below the deep chlorophyll maximum, at depth ranges from 70 m to 175 m. In addition, the species demonstrates a broad tolerance to temperature (13.9–21.08 °C) and dissolved oxygen concentrations (200.53–262.7 µmol/kg), while its occurrence seems to coincide with salinity values ranging from 34.12 psu to 36.74 psu. Unfortunately, due to our rather limited environmental dataset, no additional interpretation in relation to its ecological preferences can be made. Yet, the appearance of a single specimen of *C. curvus* sp. nov. in the surface waters off Bergen, Norway, may further suggest that the species can occur in both polar surface and the LPZ sub-tropical waters, a pattern which has already been observed in *Calciopappus caudatus, Algirosphaera robusta* (Lohmann) Norris and species belonging to the genus *Ericiolus* Thomsen *emend.* Archontikis & Young (Archontikis et al., 2023). Clearly, further comprehensive sampling of the LPZ coccolithophore community will shed light into the ecology of *C. curvus* sp. nov.

4. Material & Methods

Sample Source: The studied specimens have been collected from various environments (Fig. 4) and during different periods and programmes of sampling. In the Northwestern Mediterranean Sea, samples were taken during the cruises FRONTS-95 (17–23 June 1995) and MESO-96 (18 June – 3 July 1996) of the Institut de Ciències del Mar (ICM, CSIC) on board the R/V *García del Cid* in the North-western Mediterranean Sea (see details in Cros & Fortuño, 2002), and MATER-II (26 September – 6 October 1999) of the R/V *Hesperides* in the North-western Mediterranean and Alboran Seas (Font, 1999). Water samples were also collected in December–January 2001/2002 aboard the R/V *Sonne* during the SO-161-5 cruise (Wiedicke et al., 2002) and in October–November 2004 during BIOSOPE cruise of the R/V *L'Atalante* (Claustre and Sciandra, 2004) to the South-eastern Pacific Ocean.

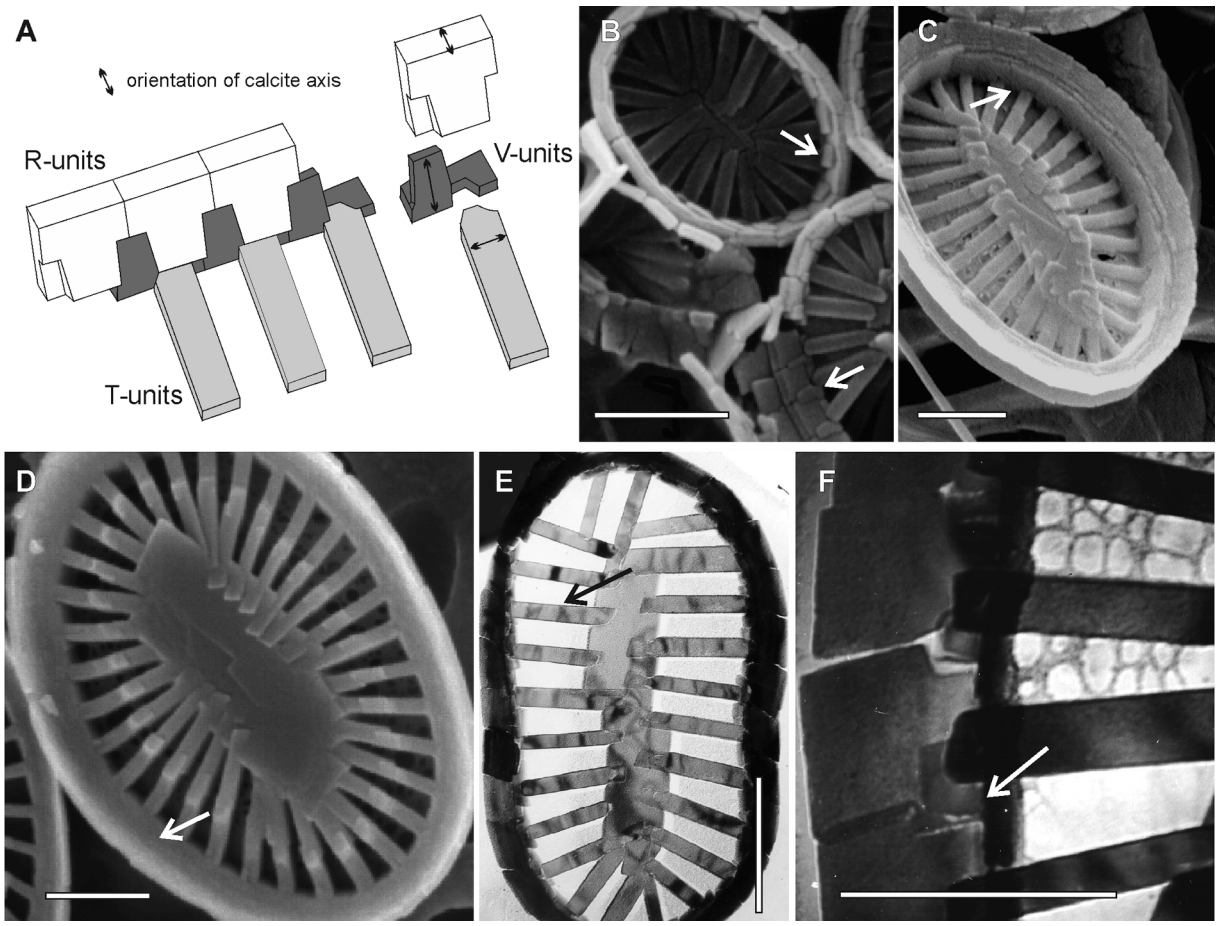

Fig. 10. Syracosphaeraceae coccolith ultrastructure. Scale bar = 0.5 μm (Figs B–F). (A). Schematic representation of the V-, R- and T-units shown in body coccoliths of *Ophiaster formosus* Gran, redrawn from Bown et al. (2017). (B). SEM image and detail view of *Ophiaster hydroideus* Lohmann body coccoliths. Arrows indicate the small V-unit elements of the inner rim cycle that interdigitate with the R-units of the outer rim cycle. Image code: 44–31 (Sample 11290/2/11, North Atlantic, 26.17°N, –30°E, 35 m, R/V *Discovery*). (C). Detail view of a body coccolith of *Michaelsarsia elegans*. Arrow indicates the presence of V-units forming an inner rim cycle. Image code: 135–21 (Station 69–11, October 1999, MATER II cruise, 37.401°N, –0.4199°E, Northwestern Mediterranean & Alboran Seas, 42.5 m). (D). SEM micrograph and detail view of a *Syracosphaera anthos* body coccolith with a slightly vaulted and lath-made ridge at the central area. This is connected to the inner rim cycle (arrow) via T-unit laths. Image code: N10U2 (Sample Nu2u/10, South Atlantic, –29°N, –13°E, 3055 m). (E). Transmission electron microscope (TEM) image of a *C. rigidus* body coccolith showing laths radially oriented and prominent gaps between them (arrow). Image code: 77073 (Station CR3, 16 September 1999, 11.86°N, 109.21°E, Cam Ranh Bay, 5 m). (F). Detail view of a *C. rigidus* body coccolith, showing the outer rim wall formed of rectangular (R-unit) elements, and the inner rim wall (arrow) made by smaller (V-unit) crystal elements. Image code: 77053 (Station CR3, 16 September 1999, 11.86°N, 109.21°E, Cam Ranh Bay, 5 m).

Additional material originates from the LPZ of the eastern Indian Ocean, off Indonesia that was collected during the geological cruise SO-184-3 (8 July – 13 September 2005) of the R/V *Sonne* (Hebbeln, 2005), and from the surface waters off Bergen, Norway in October 2008 with the use of a bucket. Samples were also obtained from sub-surface waters from Hydrostation 'S' below the deep chlorophyll maximum during a Bermuda Atlantic Time-series Study (BATS) cruise in October–November 2020 of the R/V *Atlantic Explorer* to the Sargasso Sea, North Atlantic Ocean. Information on the sample source and environmental parameters is analytically displayed in Table 1.

Filtering process and SEM: On each cruise, seawater samples were collected using a rosette with Niskin bottles attached to a Conductivity-Temperature-Depth (CTD) probe. For each sample, approximately 0.5–8 litres of seawater (see Table 1 for details) were filtered with the use of a vacuum pump onto filter membranes of five types: (1) Whatman membrane track-etched filters (0.8 μm and 1.0 μm porosity, 25 mm diameter); (2) Sartorius fleece-supported regenerated cellulose nitrate filters (0.45 μm porosity, 47 mm diameter); (3) Isopore hydrophilic, nonsterile membranes (0.8 μm porosity, 47 mm diameter); (4) Pall Life Sciences Supor-800 filter membranes (0.8 μm porosity, 25 mm diameter); and (5) Poretics OSMONICS Inc. polycarbonate filters (1 μm porosity, 25 mm diameter). On BATS cruise, samples were prefiltered using a 50 μm opening size nytex mesh to remove larger particles and contaminants. During FRONTS-95 and MESO-96, a Millipore cellulose acetate filter membrane of 3.0 μm porosity was placed below the original filter to allow for even distribution of the material. During the filtration process, filter membranes were thoroughly rinsed with either buffered distilled water (adjusted with NaOH, pH c. 8.0), bottled water (pH = 7.9–8.3) or a 20 mM sodium carbonate solution (Na_2CO_3, 2 g/L; pH c. 10) to remove salt crystals. The filters were then put into Millipore plastic Petri-dishes and were either left at room temperature or placed in an oven at 40–50 °C, for at least an hour, to dry. A portion of each filter was subsequently cut out and mounted onto a stub, sputter-coated with gold or gold–palladium and examined via electron microscopy using the following types of SEM: (1) Hitachi S-570 SEM at the facilities of ICM, CSIS, Spain; (2) VEGA3 TESCAN SEM at the Department of Earth and Environmental Systems, Indiana State University, USA; (3) FEI Sirion 200 field emission SEM at Bundesanstalt für Geowissenschaften und Rohstoffe (BGR) of the Federal Institute for Geosciences and Natural Resources, Germany; (4) Zeiss Supra 55VP SEM at the Bergen University

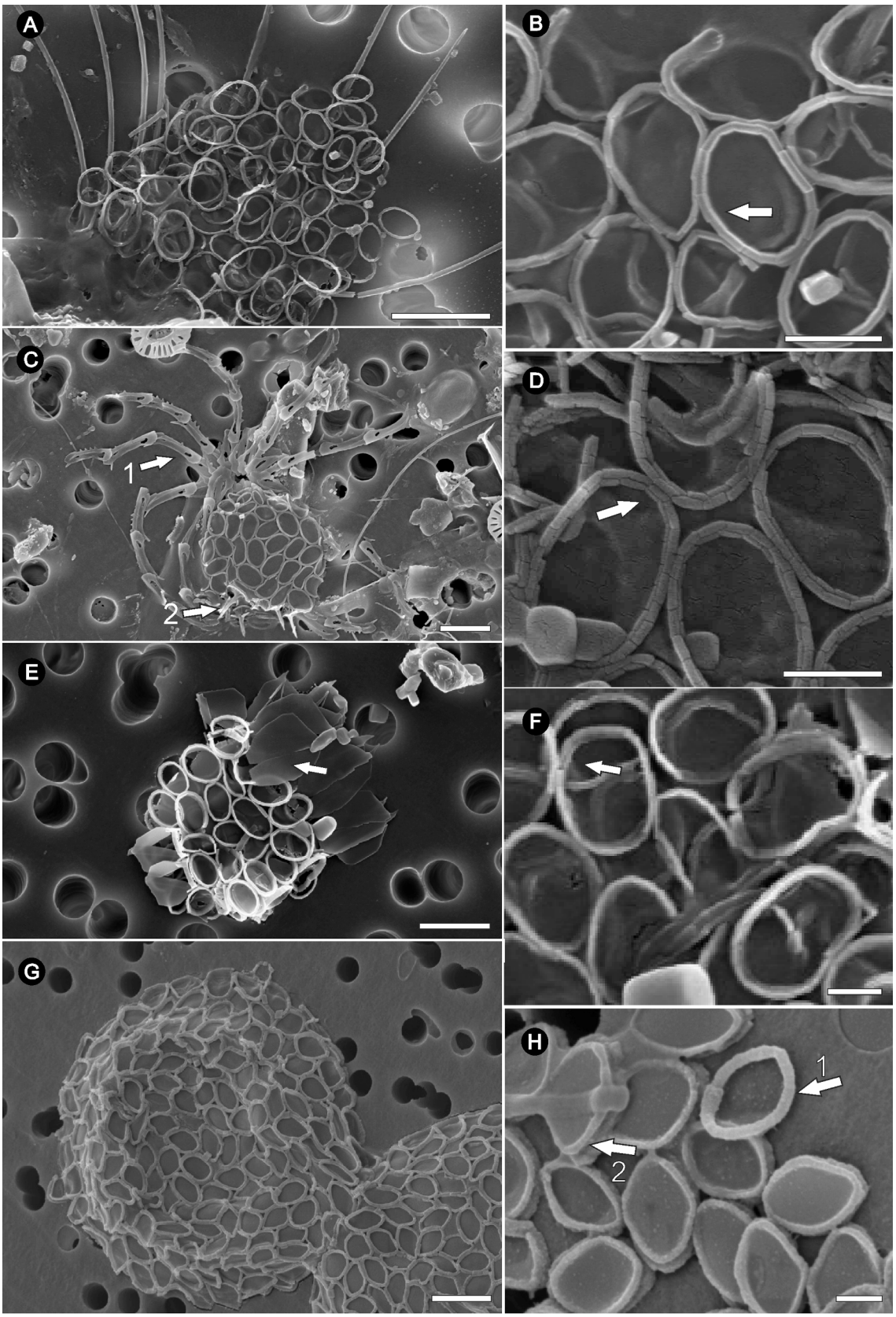

(caption on next page)

Fig. 11. Comparison and SEM micrographs of *Calciopappus curvus* sp. nov., (Figs A–B), *Ophiaster minimus* (Figs C–D), *Wigwamma annulifera* (Figs E–F) and *Jomonlithus littoralis* (Figs G–H). Scale bar = 2 μm (Figs A, C, E, G) and 0.5 μm (Figs B, D, F, H). (A). Coccosphere of *C. curvus* sp. nov., with lightly calcified body coccoliths and appendage coccoliths. Image code: Calciopunknown1. (B). Detail view of Fig. A, showing body coccoliths with an open central area and a rim formed by a single cycle of microcrystals. Image code: Calciopunknown2. (C). Well-preserved coccosphere of *O. minimus* bearing body coccoliths, circum-flagellar coccoliths and appendage coccoliths. Arrow 1 indicates the antapical strings of coccoliths (osteoliths) and arrow 2, the short spine at the central area of the circum-flagellar coccolith observed in the apical side of the coccosphere. Image code: MHeldal-Alge-26, Bergen Fjord, 60.4°N, –5.3°E, depth 0 m. (D). Detail view of an *O. minimus* specimen showing body coccoliths with an open central area and a rim formed of two cycles of microcrystals. Image code: MHeldal-002detailV, Bergen Fjord, 60.4°N, –5.3°E, depth 0 m. (E). Complete coccosphere of *W. annulifera*; arrow indicates the wigwam-like structure of the circum-flagellar coccoliths. Image code: MHeldal-6, October 2008, station Alge-6, 80°N, 22°E, Svalbard, depth 0 m. (F). Detail view of a coccosphere with open-central-area body coccoliths. Arrow indicates that the body coccolith rim is formed from a simple ring of upward growing microcrystals almost forming a tube. Image code: MHeldal-11, October 2008, station Alge–6, 80°N, 22°E, Svalbard, depth 0 m. (G). Complete coccosphere of *J. littoralis*. Image code: 228–45a, Algobank culture collection. (H). Detail view of a *J. littoralis* specimen showing body coccoliths with a rim formed of a single cycle of elements that develops into a distal (arrow 1) and a slight proximal (arrow 2) flange.

Laboratory for Electron Microscopy; and (5) Phillips XL-30 FEG and Zeiss Ultra Plus Field Emission SEM at the Natural History Museum London (NHM), UK.

Morphology, Terminology and Biometry: With regard to morphological descriptions, we followed the terminology guidelines of Young et al. (1997) with the addition of terms introduced by Young et al. (2009) for *Calciopappus, Michaelsarsia* and *Ophiaster*. The classification scheme of extant Haptophyta by Jordan et al. (1995), Young et al. (2003) and Jordan et al. (2004) is herein followed. Biometric measurements on the digital images were carried out using the image-analysis software programme ImageJ (Schneider et al., 2012). Morphometric diagrams were produced using the R package ggplot2 (Wickham, 2009).

CRediT authorship contribution statement

Odysseas A. Archontikis: Conceptualization, Methodology, Investigation, Visualization, Data curation, Formal analysis, Resources, Funding acquisition, Writing – original draft, Writing – review & editing. **Josué G. Millán:** Conceptualization, Investigation, Resources, Funding acquisition, Writing – review & editing. **Harald Andruleit:** Investigation, Resources, Writing – review & editing. **Lluïsa Cros:** Investigation, Supervision, Resources, Funding acquisition, Writing – review & editing. **Annelies Kleijne:** Validation, Supervision, Resources, Funding acquisition, Writing – review & editing. **Mikal Heldal:** Investigation, Resources, Writing – review & editing. **Hai Doan-Nhu:** Investigation, Resources, Funding acquisition, Writing – review & editing. **Amos Winter:** Investigation, Resources, Funding acquisition, Writing – review & editing. **Leocadio Blanco-Bercial:** Investigation, Resources, Funding acquisition, Writing – review & editing. **Jeremy R. Young:** Conceptualization, Validation, Investigation, Resources, Supervision, Funding acquisition, Writing – review & editing.

Declaration of Competing Interest

The authors declare that they have no known competing financial interests or personal relationships that could have appeared to influence the work reported in this paper.

Acknowledgements

We are thankful to the fellow scientists and crew of the R/V *Atlantic Explorer*, R/V *García del Cid,* R/V *Hesperides*, R/V *L'Atalante* and R/V *Sonne* for their valuable assistance in collecting seawater samples. We gratefully acknowledge Markus Geisen, Andy Howard, Sandra Broerse, Daniel Vaulot and Laura Arin for their help in obtaining samples. Special thanks are due to José-Manuel Fortuño and Maximino Delgado for kindly providing the SEM image illustrated in Fig. 1A.1. We also extend our gratitude to Innes Clatworthy, Alex Ball, Jeffery Stone and José-Manuel Fortuño for their assistance with the SEM, and to Giles Miller and Barrett Brookes for cataloguing our material at, respectively, the Natural History Museum London, UK, and the US National Herbarium of the Smithsonian Institute. The handling editor, Wiebe H.C.F Kooistra, and the three anonymous reviewers are warmly thanked for their careful perusal of our article and the thoughtful suggestions.

This study is a contribution to the EC-TMR research project CODENET, Coccolithophorid Evolutionary Biodiversity and Ecology Network (contract no. ERB-FRMX-CT97-0113) and the Bermuda Institute of Ocean Sciences (BIOS) Grant-in-Aid awarded to JGM. Part of this study is also a contribution to the Bermuda Biodiversity Project (BBP), Bermuda Aquarium, Museum and Zoo, Department of Environment & Natural Resources (special permit no. SP201201). Partial support has been provided by the NASA Indiana Space Grant Consortium (award no. 80NSSC20M0121) via a Doctoral Fellowship to JGM (US), HICCUP (RTI2018-095083-B-100) from MICINN (Spain) to LC, WOTRO Science for Global Development URG W84-76 (The Netherlands) to AK and the Viet Nam Academy of Science and Technology (grant no. NVCC17.02/22-23) to HDN. JGM, AW and LBB acknowledge the Bermuda Atlantic Time-series Study (BATS; NSF OCE-1756105 and OCE-2122606) and the Simons Foundation International (BIOSSCOPE). OAA acknowledges an INA Foundation Katharina von Salis Graduate Fellowship. This work was supported by the UK Natural Environment Research Council under grant no. NE/S007474/1 to OAA.

Appendix A. Supplementary material

Supplementary material to this article can be found online at https://doi.org/10.1016/j.protis.2023.125983.

References

Andruleit, H., Rogalla, U., Staeger, S., 2005. Living coccolithophores recorded during the onset of upwelling conditions off Oman in the western Arabian Sea. Journal of Nannoplankton Research 27, 1–14.

Archontikis, O.A., Millán, J.G., Winter, A., Young, J.R., 2023. Taxonomic re-evaluation of *Ericiolus* and *Mercedesia* (Prymnesiophyceae) and description of three new species. Phycologia 62, 179–193.

Archontikis, O.A., Young, J.R., Cros, L., 2020. Taxonomic revision and classification of extant holococcolithophores previously placed in the genus *Anthosphaera* Kamptner emend. Kleijne 1991. Acta Protozoologica 59, 121–139.

Aubry, M.-P., 2009. A sea of Lilliputians. Palaeogeography Palaeoclimatology Palaeoecology 284, 88–113.

Bendif, E.M., Probert, I., Archontikis, O.A., Young, J.R., Beaufort, L., Rickaby, R.E., Filatov, D., 2023. Rapid diversification underlying the global dominance of a cosmopolitan phytoplankton. The ISME Journal 17, 630–640.

Bown, P.R., Lees, J.A., Young, J.R., 2017. On the Cretaceous origin of the Order Syracosphaerales and the genus *Syracosphaera*. Journal of Micropalaeontology 36, 153–165.

Cavalier-Smith, T., Allsopp, M., Häuber, M., Gothe, G., Chao, E., Couch, J., Maier, U.-G., 1996. Chromobiote phylogeny: the enigmatic alga *Reticulosphaera japonensis* is an aberrant haptophyte, not a heterokont. European Journal of Phycology 31, 255–263.

Claustre H, Sciandra A (2004) BIOSOPE cruise, RV L'Atalante.

Cros, L., Fortuño, J.-M., 2002. Atlas of northwestern Mediterranean coccolithophores. Scientia Marina 66 (Suppl.1), 186.

Edvardsen, B., Eikrem, W., Green, J.C., Andersen, R.A., Moon-Van Der Staay, S.Y., Medlin, L.K., 2000. Phylogenetic reconstructions of the Haptophyta inferred from 18S ribosomal DNA sequences and available morphological data. Phycologia 39, 19–35.

Font J (1999) BIO Hesperides: MATER-2 (leg 3): HE059: Informe de Campaña.

Gaarder, K.R., 1967. Observations on the genus *Ophiaster* Gran (Coccolithineae). Sarsia 29, 183–192.

Gaarder, K.R., Markali, J., Ramsfjell, E., 1954. Further observations on the coccolithophorid *Calciopappus caudatus*. Avhandlinger utgitt av det Norske Videnskapsakademi i Oslo. Mat.- Naturvid. Klasse 1, 1–9.

Gaarder, K.R., Ramsfjell, E., 1954. A new coccolithophorid from northern waters, *Calciopappus caudatus*. n. gen., n. sp. Nytt Magasin for Botanikk 2, 155–156.
Hay, W.W., 1977. Calcareous nannofossils. In: Ramsay, A.T.S. (Ed.), Oceanic Micropalaentology. Academic Press, London, pp. 1055–1200.
Hebbeln D (2005) Cruise Report: PABESIA, RV Sonne Cruise SO-184. Cilacap-Darwin, Durban (8 July–13 September 2005).
Heimdal, B.R., Gaarder, K.R., 1981. Coccolithophorids from the northern part of the eastern central Atlantic II. Heterococcolithophorids. "Meteor" Forschungsergebnisse. Reihe D. Biologie 33, 37–69.
Hibberd, D.J., 1972. Chrysophyta: definition and interpretation. British Phycological Journal 7, 281.
Hibberd, D.J., 1976. The ultrastructure and taxonomy of the Chrysophyceae and Prymnesiophyceae (Haptophyceae): a survey with some new observations on the ultrastructure of the Chrysophyceae. Botanical Journal of the Linnean Society 72, 55–80.
Inouye, I., Chihara, M., 1983. Ultrastructure and taxonomy of *Jomonlithus littoralis* gen. et sp. nov. (Class Prymnesiophyceae), a coccolithophorid from the Northwest Pacific. Botanical Magazine. Tokyo 96, 365–376.
Inouye, I., Pienaar, R.N., 1988. Light and electron microscope observations of the type species of *Syracosphaera, S. pulchra* (Prymnesiophyceae). British Phycological Journal 23, 205–217.
Jordan, R.W., Cros, L., Young, J.R., 2004. A revised classification scheme for living Haptophytes. Micropaleontology 50, 55–79.
Jordan, R.W., Kleijne, A., Heimdal, B.R., Green, J.C., 1995. A glossary of the extant Haptophyta of the world. Journal of the Marine Biological Association of the United Kingdom 75, 769–814.
Keuter, S., Young, J.R., Koplovitz, G., Zingone, A., Frada, M.J., 2021. Novel heterococcolithophores, holococcolithophores and life cycle combinations from the families Syracosphaeraceae and Pappposphaeraceae and the genus Florisphaera. Journal of Micropalaeontology 40, 75–99.
Kleijne, A., Cros, L., 2009. Ten new extant species of the coccolithophore *Syracosphaera* and a revised classification scheme for the genus. Micropaleontology 55, 425–462.
Konno, S., Jordan, R.W., 2006. Lagoon coccolithophorids from the Republic of Palau, NW Equatorial Pacific. Journal of Nannoplankton Research 28, 95–110.
Lemmermann, E., 1903. Das Phytoplankton des Meeres. II. Naturwissenschaftlicher Verein zu Bremen. Abhandlungen 17, 341–418.
Lohmann, H., 1902. Die Coccolithophoridae, eine Monographie der Coccolithen bildenden Flagellaten, zugleich ein Beitrag zur Kenntnis des Mittelmeerauftriebs. Archiv für Protistenkunde 1, 89–165.
Manton, I., Bremer, G., Oates, K., 1984. Nanoplankton from the Galapagos Islands: *Michaelsarsia elegans* Gran and *Halopappus adriaticus* Schiller (coccolithophorids) with special reference to coccoliths and their unmineralized components. Philosophical Transactions of the Royal Society of London (B) B 305, 183–199.
Manton, I., Oates, K., 1983. Nanoplankton from the Galapagos Islands: Two genera of spectacular coccolithophorids (*Ophiaster* and *Calciopappus*) with special emphasis on unmineralized periplast components. Philosophical Transactions of the Royal Society of London (B) 300, 435–462.
Manton, I., Sutherland, J., Oates, K., 1977. Arctic coccolithophorids: *Wigwamma arctica* gen. et sp. nov. from Greenland and Arctic Canada; *W. annulifera* sp. nov. from South Africa and S. Alaska and *Calciarcus alaskensis* gen. et sp. nov. from S. Alaska. Proceedings of the Royal Society of London 197, 145–168.
Medlin, L.K., Sáez, A.G., Young, J.R., 2008. A molecular clock for coccolithophores and implications for selectivity of phytoplankton extinctions across the K/T boundary. Marine Micropaleontology 67, 69–86.
Monteiro, F., Bach, L.T., Brownlee, C., Bown, P.R., Rickaby, R.E.M., Poulton, A.J., Tyrrell, T., Beaufort, L., Dutkiewicz, S., Gibbs, S.J., Gutowsska, M.A., Lee, R., Riebesell, U., Young, J.R., Ridgwell, A., 2016. Why marine phytoplankton calcify. Science Advances 2016, 1–14.
Poulton, A.J., Adey, T.R., Balch, W.M., Holligan, P.M., 2007. Relating coccolithophore calcification rates to phytoplankton community dynamics: Regional differences and implications for carbon export. Deep Sea Research Part II: Topical Studies in Oceanography 54, 538–557.
Probert, I., Fresnel, J., Young, J.R., 2014. The life cycle and taxonomic affinity of the coccolithophore *Jomonlithus littoralis* (Prymnesiophyceae). Cryptogamie, Algologie 35, 389–405.
Schlitzer R (2021) Ocean data view. https://odv.awi.de.
Schneider, C.A., Rasband, W., Eliceiri, K.W., 2012. NIH Image to ImageJ: 25 years of image analysis. Nature Methods 9, 671–675.
Thomsen, H.A., 1980. *Wigwamma scenozonion* sp. nov. (Prymnesiophyceae) from West Greenland. British Phycological Journal 15, 335–342.
Thomsen, H.A., 2016. Baltic Sea coccolithophores – an overview of insights into their taxonomy and ecology from the last 40 years. Journal of Nannoplankton Research 36, 97–119.
Thomsen, H.A., Buck, K.R., Coale, S.L., Garrison, D.L., Gowing, M.M., 1988. Nanoplanktonic coccolithophorids (Prymnesiophyceae, Haptophyceae) from the Weddell Sea, Antarctica. Nordic Journal of Botany 8, 419–436.
Thomsen, H.A., Ostergaard, J.B., Heldal, M., 2013. Coccolithophorids in polar waters: *Wigwamma* spp. revisited. Acta Protozoologica 52, 237–256.
Tyrrell, T., Young, J.R., 2009. Coccolithophores. In: Steele, J.H., Turekian, K.K., Thorpe, S.A. (Eds.), Encyclopedia of Ocean Sciences. Academic Press, San Diego, US, pp. 3568–3576.
Wallich, G.C., 1877. Observations on the coccosphere. Annals and Magazine of Natural History 19, 342–350.
Wickham, H., 2009. Elegant graphics for data analysis (ggplot2). Applied Spatial Data Analysis R.
Wiedicke, M., Andruleit, H., Balmaceda, G., Bruns, A., Contardo, X., Cramer, B., Delisle, G., Diaz-Naveas, J., Erbacher, J., Fenner, J., Goergens, R., Gomez, C., Harazim, B., Heubeck, C., Kloep, F., Kramer, W., Kus, J., Lückge, A., Mohtadi, M., Mühr, P., Panten, D., Reinhardt, L., Steinmann, D., Stummeyer, J., Zeibig, Z., 2002. Cruise Report Sonne Cruise SO-161-5, SPOC, Subduction Processes off Chile. BGR Reports 11241/02, BGR Reports. Bundesanstalt fuer Geowissenschaften und Rohstoffe, Hannover.
Young, J.R., Andruleit, H., Probert, I., 2009. Coccolith function and morphogenesis, insights from appendage-bearing coccolithophores of the family Syracosphaeraceae (Haptophyta). Journal of Phycology 45, 213–226.
Young, J.R., Bergen, J.A., Bown, P.R., Burnett, J.A., Fiorentino, A., Jordan, R.W., Kleijne, A., van Niel, B.E., Romein, A.J.T., von Salis, K., 1997. Guidelines for coccolith and calcareous nannofossil terminology. Palaeontology 40, 875–912.
Young JR, Bown PR, Lees JA (2023) Nannotax3 website. International Nannoplankton Association. Accessed 10 January 2023. URL: www.mikrotax.org/Nannotax3.
Young, J.R., Davis, S.A., Bown, P.R., Mann, S., 1999. Coccolith ultrastructure and biomineralisation. Journal of Structural Biology 126, 195–215.
Young, J.R., Didymus, J.M., Bown, P.R., Prins, B., Mann, S., 1992. Crystal assembly and phylogenetic evolution in heterococcoliths. Nature 356, 516–518.
Young, J.R., Geisen, M., Cros, L., Kleijne, A., Probert, I., Ostergaard, J.B., 2003. A guide to extant coccolithophore taxonomy. Journal of Nannoplankton Research, Special Issue 1, 1–132.
Young, J.R., Geisen, M., Probert, I., 2005. A review of selected aspects of coccolithophore biology with implications for palaeobiodiversity estimation. Micropaleontology 51, 267–288.
Young, J.R., Henriksen, K., Probert, I., 2004. Structure and morphogenesis of the coccoliths of the CODENET species. In: Thierstein, H.R., Young, J.R. (Eds.), Coccolithophores – From molecular processes to global impact. Springer, pp. 191–216.
Young, J.R., Liu, H., Probert, I., Aris-Brosou, S., de Vargas, C., 2014. Morphospecies versus phylospecies concepts for evaluating phytoplankton diversity: The Case of the Coccolithophores. Cryptogamie, Algologie 35, 353–377.